


Cite this: *RSC Adv.*, 2018, 8, 3663

Synthesis, characterisation and ion-binding properties of oxathiacrown ethers appended to $[\text{Ru}(\text{bpy})_2]^{2+}$. Selectivity towards Hg^{2+} , Cd^{2+} and Pb^{2+} †

Ruth A. Odhiambo,^{ab} Austin O. Aluoch,^{id} Lydia W. Njenga,^a Stanley M. Kagwanja,^c Shem O. Wandiga^{id} and Ola F. Wendt^{id}*^{ab}

A series of complexes with oxathiacrown ethers appended to a $[\text{Ru}(\text{bpy})_2]^{2+}$ moiety have been synthesized and characterised using ^1H NMR, ^{13}C NMR, IR, electronic absorption and emission spectroscopies, mass spectrometry and elemental analyses. The complexes exhibit strong MLCT luminescence bands in the range 608–611 nm and one reversible metal centred oxidation potential in the range 1.00–1.02 V. Their selectivity and sensitivity towards Hg^{2+} , Cd^{2+} and Pb^{2+} metal ions have been investigated using electronic absorption, luminescence, cyclic and differential pulse voltammetry titrations. Their responses towards selected cations and anions have also been investigated using electronic absorption and luminescence. While the complexes are selective towards Hg^{2+} and Cd^{2+} ions, none of them is selective towards Pb^{2+} ions. In particular, complex **2** gives a selective change in the UV/Vis absorbance with Hg^{2+} making it possible to detect mercury down to a detection limit of 68 ppm. The binding constants and limits of detection of the complexes have been calculated, with values ranging from 4.37 to 5.38 and 1.4×10^{-3} to 6.8×10^{-5} for log K_s and LOD respectively.

Received 22nd December 2017
Accepted 12th January 2018

DOI: 10.1039/c7ra13589k

rsc.li/rsc-advances

Introduction

The presence of toxic metal ions in the environment poses great danger to humans due to their non-biodegradability and bio-accumulation. Their environmental detection will require the development of simple, highly sensitive and selective analytical methods such as artificial chemosensors and, thus, the design and synthesis of such sensors with high affinity and selectivity have been given a lot of attention.^{1–4}

Crown ethers have been extensively used as nucleating ligands and chelators for specific metal ions. Together with their analogues, they permit control of both the coordination environment (donor atoms) and in principle, the stereochemistry at a metal ion. Their selective complexing ability, which depends upon the relative size of the cavity and diameter of the cation, number of donor atoms in the crown ring and the charge of the cation has led to their use in chemosensing; this subject area has been extensively reviewed.^{5,6} The selectivity in binding metal ions can be fine-tuned either by

incorporating different soft and hard donor atoms in the chelating ring or by modifying the flexibility properties of the macrocyclic structure. This offers a tremendous potential in fabricating specific sensors for selected ions.⁷ Although a lot of work has been done on crown ether based chemosensors (CEBCs), the focus has been on hard donor systems with O and/or N and little emphasis has been put on soft-donor redox-active macrocyclic systems which have significant relevance in both industrial and environmental areas, because of their potential to sense environmentally toxic metals, which are usually soft. Relatively isolated and few systematic studies have been carried out to assess their selectivity towards a range of transition metals.^{8,9} Such systems would be expected to show enhanced binding capabilities and selectivity in comparison with the hard donor systems. In the present study, a series of oxathiacrown ether ligands (**L1–L4**) bonded to a $[\text{Ru}(\text{bpy})_2]^{2+}$ complexing unit were synthesized, characterized and their recognition ability towards Hg^{2+} , Cd^{2+} and Pb^{2+} metal ions investigated by spectroscopic and electrochemical methods. Ligand **L3** has been investigated previously but not in a comparative study with the other ligands.⁹

The $[\text{Ru}(\text{bpy})_2]^{2+}$ moiety served as a suitable signalling unit due to its strong MLCT absorption and its emitting excited states.^{10,11} It has well-defined spectroscopic, photophysical, photochemical and electrochemical properties which are

^aUniversity of Nairobi, P. O. Box 30197 – 00100, Nairobi, Kenya

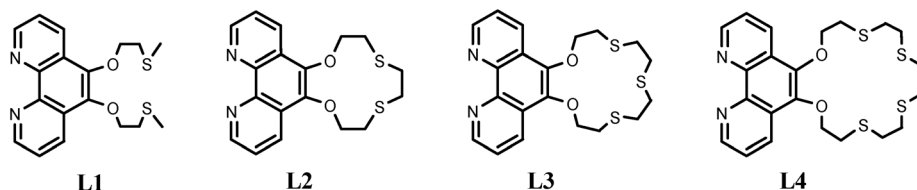
^bLund University, Box 124, Lund, Sweden. E-mail: ola.wendt@chem.lu.se

^cChuka University, P. O. Box 109 – 60400, Chuka, Kenya

^dThe Technical University of Kenya, P. O. Box 52428 – 00200, Nairobi, Kenya

† Electronic supplementary information (ESI) available. See DOI: 10.1039/c7ra13589k





sensitive to variations of external inputs, thus making it useful in the construction of supramolecular systems in sensor applications.^{12,13} The results obtained will further enhance the understanding of the complexation behaviour and ability of such systems to selectively bind and recover soft toxic metals that have potentially adverse effects on health.

Experimental section

Materials and measurements

Commercial reagents were used as supplied without further purification. Reagents which are not commercially available were prepared using established literature methods with modifications; 3,6-dithiaoctane-1,8-dithiol,^{14,15} 3,8-dithiaoctane-1,8-diol,¹⁶ mesylate and dimesylates,¹⁷ 1,10-phenanthroline-5,6-dione,¹⁸ 5,6-dihydroxy-1,10-phenanthroline¹⁹ and Ru(bpy)₂Cl₂·2H₂O.²⁰ Ruthenium complexes were synthesized using modified literature procedures.⁹ Dry organic solvents were obtained from a dry solvent dispenser. Sample purification through flash column chromatography was done using neutral alumina or silica gel while the progress of reactions was monitored through thin layer chromatography (TLC) with Al₂O₃ neutral (type T 150 F₂₅₄) or silica gel 60 (F₂₅₄) plates.

Microanalytical experiments (C, H, N analysis) were performed by Mikroanalytisches Laboratorium Kolbe, Mülheim an der Ruhr, Germany. Mass spectra were recorded on Micromass Q-TOF Micromass spectrometer while infrared spectra were obtained in solution using a Bruker Alpha FTIR spectrometer. Electronic absorption and luminescence spectra were recorded on a Varian Cary 100 Bio UV/Vis- and Varian Cary Eclipse fluorescence-spectrophotometer, respectively. Luminescence quantum yields were measured in optically dilute solutions, using [Ru(bpy)₃]²⁺ as the reference emitter ($\Phi = 0.04$ in water).²¹ The different refractive indices for the luminescence standard and sample solvent were corrected for. ¹H NMR and ¹³C NMR spectra were obtained on a Bruker Ultrashield Plus Avance 400 MHz spectrometer and the chemical shifts are reported relative to TMS. All the electrochemical experiments were performed on an Autolab potentiostat/galvanostat (PGSTAT30). The measurements were carried out using a three-electrode cell configuration with a platinum disk working electrode, platinum gauze counter electrode and Ag/0.01 M AgNO₃ reference electrode. Solutions of the complexes in acetonitrile containing 0.1 M tetrabutylammonium hexafluoro phosphate as supporting electrolyte were deoxygenated prior to each experiment. Binding constants²² and limits of detection²³ were calculated according to literature methods.

Syntheses

2-(methylthio)ethylmesylate. A mixture of 2-(methylthio)ethanol (1.8 ml, 20 mmol), pyridine (4.0 ml, 50 mmol) and dry

CH₂Cl₂ (40 ml) was charged into a flask and methanesulfonyl chloride (2.3 ml, 30 mmol) in CH₂Cl₂ (10 ml) was added dropwise at 0 °C. The reaction mixture was allowed to warm to ambient temperature, stirred for 10 h and the mixture poured into water. The organic layer was separated while the aqueous layer was extracted with chloroform once. The combined organic phases were evaporated *in vacuo*, THF (3 × 100 ml) added and filtration was performed to remove the insoluble pyridinium salt. The filtrate was evaporated under reduced pressure to yield a colourless oil. Yield: 1.47 g (42%). ¹H NMR (400 MHz, CDCl₃): δ = 3.61 (m, 2H, OCH₂), 2.80 (t, 2H, SCH₂), 2.12 (s, 6H, CH₃). ¹³C NMR: 42.7 (OCH₂), 36.1 (SCH₂), 32.2 (CH₃). IR (cm⁻¹): 1350, 1173 (CH₃-SO₂), 685 (CH₂-S-CH₂).

5,6-Bis(2-methylthioethoxy)-1,10-phenanthroline (L1). A mixture of 1,10-phenanthroline-5,6-diol (0.25 g, 1.2 mmol), 2-(methylthio)ethyl mesylate (0.7 g, 4 mmol) and K₂CO₃ (0.6 g, 4 mmol) was dissolved in dry DMF (50 ml) in a dry two-necked flask fitted with a reflux condenser under nitrogen gas. The suspension was gently purged with nitrogen for 5 min and then heated to 80 °C for 18 h. After the reaction was complete, the mixture was cooled down to room temperature and filtered to remove inorganic salts. The filtrate was evaporated *in vacuo*, the crude product dissolved in CH₂Cl₂ (50 ml) and washed with brine (2 × 50 ml). The organic layer was dried over MgSO₄, evaporated *in vacuo* and the crude product purified by column chromatography with alumina as the stationary phase using CH₂Cl₂/methanol (98 : 2) as the eluent to afford a red solid. Yield: 0.12 g (30%). ¹H NMR (400 MHz, CDCl₃): δ = 9.15 (m, 2H, phen), 8.70 (m, 2H, phen), 7.68 (m, 2H, phen), 4.47 (m, 4H, OCH₂), 3.02 (dd, 4H, SCH₂, J_1 = 8.3 Hz, J_2 = 4.7 Hz), 2.25 (s, 6H, CH₃); ¹³C NMR: 149.4, 144.5, 142.0, 130.5, 125.9, 123.2 (phen); 72.4 (OCH₂), 34.3 (SCH₂), 16.2 (CH₃). IR (cm⁻¹): 1668 (C=N), 681 (CH₂-S-CH₂). ESI-MS: m/z calcd (found) 361.1039 (361.1043) ([M + H]⁺).

3,6-Dithiaoctane-1,8-diol. A three-necked round bottom flask fitted with a reflux condenser was flushed with nitrogen gas and then charged with ethanol (100 ml) which was mechanically stirred while sodium metal (2.95 g, 128 mmol) was cautiously added. After the sodium was dissolved, the solution was warmed to 45–50 °C and a solution of ethane-1,2-dithiol (5.1 ml, 60 mmol) in ethanol (10 ml) added dropwise over a period of 15 min. A solution of 2-chloroethanol (8.6 ml, 128 mmol) in ethanol (10 ml) was then added dropwise to the resulting solution and the reaction mixture refluxed for 4 h. On cooling to room temperature, it was filtered and the filtrate evaporated *in vacuo* to dryness, giving a white solid which was triturated with diethyl ether and dried under vacuum. Yield: 10.8 g (97%). ¹H NMR (400 MHz, CDCl₃): δ = 3.77 (dd, 4H, OCH₂), 2.81–2.76 (m, 8H, SCH₂), 2.25 (s, 2H, OH); ¹³C NMR: 60.7 (CH₂OH), 35.5



(SCH₂), 32.0 (SCH₂), 30.9 (SCH₂). IR (cm⁻¹): 3361 (OH), 689 (CH₂-S-CH₂).

3,6-Dithiaoctane-1,8-dimesylate. This compound was prepared following a procedure similar to the synthesis of 2-(methylthio)ethylmesylate using 3,6-dithiaoctane-1,8-diol (3.64 g, 20 mmol), pyridine (8.0 ml, 0.1 mol) and methanesulfonyl chloride (4.6 ml, 60 mmol). The mixture was stirred for 3 h. Subsequent purification gave a pale yellow oil which formed a white solid on standing. Yield: 4.72 g (70%). ¹H NMR (400 MHz, CDCl₃): δ = 3.66 (m, 4H, OCH₂), 2.96–2.89 (m, 8H, SCH₂), 2.81 (s, 6H, CH₃); ¹³C NMR: 43.1 (OCH₂), 39.6 (SCH₂), 34.4 (SCH₂), 32.6 (CH₃). IR (cm⁻¹): 1352, 1173 (CH₃-SO₂), 677 (CH₂-S-CH₂).

1,10-Dioxa-4,7-dithiacyclobutaoctano[2,3-*f*][1,10]-phenanthroline (L2). A mixture of 1,10-phenanthroline-5,6-diol (0.17 g, 0.8 mmol), 3,6-dithiaoctane-1,8-dimesylate (0.26 g, 0.8 mmol) and Cs₂CO₃ (0.75 g, 2.4 mmol) in dry DMF (40 ml) was added into a pre-dried Schlenk tube under an atmosphere of dry nitrogen. The tube was then sealed and the mixture stirred at 85 °C for 48 h. After the reaction was complete, the system was left to cool down to room temperature and filtered to remove inorganic salts. The filtrate was evaporated, the product obtained dissolved in CH₂Cl₂ (50 ml) and washed with brine (2 × 50 ml). The organic layer was collected, dried over MgSO₄ and evaporated under reduced pressure to give a brown oil. Purification of the product by flash column chromatography on alumina with chloroform : hexane (1 : 1, v/v) yielded a white solid. Yield: 0.14 g (50%). ¹H NMR (400 MHz, CDCl₃): δ = 9.17 (dd, 2H, phen, *J*₁ = 4.3 Hz, *J*₂ = 1.6 Hz), 8.50 (dd, 2H, phen, *J*₁ = 8.3 Hz, *J*₂ = 1.6 Hz), 7.68 (dd, 2H, phen, *J*₁ = 8.3 Hz, *J*₂ = 4.3 Hz), 4.59 (m, 2H, OCH₂), 4.46 (dt, 2H, OCH₂, *J*₁ = 12.5 Hz, *J*₂ = 6.2 Hz), 3.18 (m, 2H, SCH₂), 3.09 (d, 2H, SCH₂, *J* = 6.3 Hz), 2.96 (dd, 2H, SCH₂, *J*₁ = 10.7 Hz, *J*₂ = 7.7 Hz), 2.82 (m, 2H, SCH₂); ¹³C NMR: 149.6, 142.5, 132.8, 130.5, 128.7, 122.7 (phen); 76.1 (OCH₂), 31.7, 29.7 (SCH₂). IR (cm⁻¹): 1671 (C=N), sh (CH₂-S-CH₂). ESI-MS: *m/z* calcd (found) 359.0843 (359.0887) ([M + H]⁺).

3,6,9-Trithiaundecane-1,11-diol. This compound was prepared following a procedure similar to the synthesis of 3,6-dithiaoctane-1,8-diol using 3-thiapentane-1,5-dithiol (8.0 ml, 60 mmol) in place of ethane-1,2-dithiol. After refluxing for 4 h, the reaction mixture was cooled to room temperature, the organic layer decanted while the white residue was treated with hot acetone (100 ml) and then filtered. The organic phases were combined, evaporated to dryness and the resulting solid triturated with diethyl ether to yield a white solid. Yield: 11.24 g (76%). ¹H NMR (400 MHz, CDCl₃): δ = 3.85 (d, 4H, OCH₂, *J* = 5.1 Hz), 2.90–2.81 (m, 12H, SCH₂), 2.30 (br s, 2H, OH); ¹³C NMR: 60.7 (CH₂OH), 35.4 (SCH₂), 32.4 (SCH₂), 32.0 (SCH₂). IR (cm⁻¹): 3292 (OH), 680 (CH₂-S-CH₂).

3,6,9-Trithiaundecane-1,11-dimesylate. This compound was prepared following a procedure similar to the preparation of 3,6-dithiaoctane-1,8-dimesylate using a mixture of 3,6,9-trithiaundecane-1,11-diol (2.42 g, 10 mmol), pyridine (4.0 ml, 50 mmol) and methanesulfonyl chloride (2.3 ml, 30 mmol). Yield: 2.45 g (62%). ¹H NMR (400 MHz, CDCl₃): δ = 3.67 (m, 4H, OCH₂), 2.95–2.82 (m, 12H, SCH₂), 2.80 (s, 6H, CH₃); ¹³C NMR:

43.1 (OCH₂), 39.4 (SCH₂), 34.4 (SCH₂), 32.4 (CH₃). IR (cm⁻¹): 1348, 1152 (CH₃-SO₂), 679 (CH₂-S-CH₂).

1,13-Dioxa-4,7,10-trithiacyclopentadecano[2,3-*f*][1,10]-phenanthroline (L3). This compound was prepared following a procedure similar to the synthesis of 1,10-dioxa-4,7-dithiacyclobutaoctano [2,3-*f*][1,10]-phenanthroline using 1,10-phenanthroline-5,6-diol (0.22 g, 1 mmol), 3,6,9-trithiaundecane-1,11-dimesylate (0.4 g, 1 mmol) and Cs₂CO₃ (0.98 g, 3 mmol) in dry DMF (40 ml). Yield: 0.24 g (57%). ¹H NMR (400 MHz, CDCl₃): δ = 9.17 (dd, 2H, phen, *J*₁ = 4.5 Hz, *J*₂ = 1.7 Hz), 8.67 (m, 2H, phen), 7.69 (m, 2H, phen), 4.46 (dt, 4H, OCH₂, *J*₁ = 7.0 Hz, *J*₂ = 7.0 Hz), 3.08 (m, 4H, SCH₂), 2.95–2.78 (m, 8H, SCH₂); ¹³C NMR: 149.7, 141.7, 131.2, 130.5, 125.6, 123.3 (phen); 73.7 (OCH₂), 32.9, 31.7 (SCH₂). IR (cm⁻¹): 1695 (C=N), 674 (CH₂-S-CH₂). ESI-MS: *m/z* calcd (found) 419.0877 (419.0920) ([M + H]⁺).

3,6,9,12-Tetrathiatetradecane-1,14-diol. 3,6-dithiaoctane-1,8-dithiol was prepared by converting 3,6-dithiaoctane-1,8-diol to the dithiol according to the literature procedure.¹⁷ 3,6,9,12-Tetrathiatetradecane-1,14-diol was prepared by reacting 3,6-dithiaoctane-1,8-dithiol (2.0 g, 9 mmol) and 2-chloroethanol (1.4 ml, 21 mmol) in the same manner as 3,6-dithiaoctane-1,8-diol. Yield: 2.1 g (74%). ¹H NMR (400 MHz, CDCl₃): δ = 3.78 (t, 4H, OCH₂, *J* = 5.9 Hz), 3.12–2.76 (m, 16H, OCH₂), 2.30 (br s, 2H, OH); ¹³C NMR: 60.7 (CH₂OH), 41.8 (SCH₂), 35.4 (SCH₂), 32.4 (SCH₂), 31.9 (SCH₂), 29.7 (SCH₂). IR (cm⁻¹): 3291 (OH), 678 (CH₂-S-CH₂).

3,6,9,12-Tetrathiatetradecane-1,14-dimesylate. This compound was prepared following a procedure similar to the synthesis of 3,6-dithiaoctane-1,8-dimesylate using 3,6,9,12-tetrathiatetradecane-1,14-diol (1.6 g, 5.3 mmol), pyridine (1.3 ml, 16 mmol) and methanesulfonyl chloride (1.3 ml, 16 mmol). Yield: 1.9 g, (78%). ¹H NMR (400 MHz, CDCl₃): δ = 3.60 (m, 4H, OCH₂), 2.94 (s, 6H, CH₃), 2.84–2.72 (m, 16H, SCH₂); ¹³C NMR: 43.1 (OCH₂), 39.1 (SCH₂), 34.5 (SCH₂), 32.5 (CH₃). IR (cm⁻¹): 1345, 1171 (CH₃-SO₂), 679 (CH₂-S-CH₂).

1,15-Dioxa-4,7,10,13-tetrathiacyclohexadecano[2,3-*f*][1,10]-phenanthroline (L4). A mixture of NaH (0.10 g of 60% mineral oil dispersion, 2.5 mmol) and 1,10-phenanthroline-5,6-diol (0.25 g, 1.2 mmol) in dry DMF (20 ml) was discharged into a flask under N₂ and the mixture stirred for 10 min. A solution of 3,6,9,12-tetrathiatetradecane-1,14-dimesylate (0.55 g, 1.2 mmol) in degassed DMF (20 ml) was then added and the mixture refluxed at 80 °C for 24 h. After completion of the reaction, the reaction mixture was filtered, concentrated and water (30 ml) added. The target compound was extracted with several small portions of CH₂Cl₂, the organic phases combined, dried over MgSO₄ and evaporated under vacuum to give a brown oil. Purification by chromatography on silica using 10% methanol in dichloromethane yielded a white solid. Yield: 0.24 g (43%). ¹H NMR (400 MHz, CDCl₃): δ = 9.16 (dd, 2H, phen, *J*₁ = 4.7 Hz, *J*₂ = 1.8 Hz), 8.61 (dd, 2H, phen, *J*₁ = 7.9 Hz, *J*₂ = 1.8 Hz), 7.66 (dd, 2H, phen, *J*₁ = 7.9 Hz, *J*₂ = 4.7 Hz), 4.46 (dd, 4H, OCH₂, *J*₁ = 8.0 Hz, *J*₂ = 3.0 Hz), 3.08–2.77 (m, 16H, SCH₂); ¹³C NMR: 149.6, 142.1, 137.2, 131.2, 125.8, 122.9 (phen); 72.9 (OCH₂), 32.4, 31.6, 29.7 (SCH₂). IR (cm⁻¹): 1684 (C=N), 688 (CH₂-S-CH₂). ESI-MS: *m/z* calcd (found) 479.0911 (479.0954) ([M + H]⁺).

[Ru(bpy)₂(L1)](PF₆)₂ (1). A mixture of L1 (55 mg, 0.17 mmol) and [Ru(bpy)₂Cl₂]·2H₂O (90 mg, 0.17 mmol) in ethanol (50 ml)



was refluxed under nitrogen atmosphere until the purple coloration turned cherry red (5 h). The reaction mixture was cooled to room temperature, filtered and the solvent evaporated. The product obtained was dissolved in a minimum amount of methanol and a saturated solution of KPF₆ in methanol added to precipitate a red solid which was purified on an alumina column using acetonitrile/toluene (9 : 1, v/v), followed by recrystallization from acetonitrile/diethyl ether to afford a red microcrystalline solid. Yield: 75 mg (42%). ¹H NMR (400 MHz, CD₃CN): δ = 8.89 (m, 2H, phen), 8.53 (dd, 4H, bpy, *J*₁ = 11.0 Hz, *J*₂ = 8.3 Hz), 8.12 (td, 2H, bpy, *J*₁ = 8.1 Hz, *J*₂ = 8.0 Hz, *J*₃ = 1.5 Hz), 8.02 (m, 4H, bpy), 7.83 (d, 2H, phen, *J* = 5.6 Hz), 7.74 (m, 2H, bpy), 7.57 (d, 2H, phen, *J* = 4.4 Hz), 7.46 (dd, 2H, bpy, *J*₁ = 9.7 Hz, *J*₂ = 3.6 Hz), 7.26 (m, 2H, bpy), 4.53 (t, 4H, OCH₂, *J* = 5.0 Hz), 3.04 (m, 4H, SCH₂), 2.21 (s, 6H, CH₃); ¹³C NMR: 156.7, 153.3, 151.5, 137.8, 136.4, 131.5, 127.4, 126.7, 125.7, 124.3, 122.9 (phen/bpy), 72.9 (OCH₂), 33.5 (SCH₂), 15.0 (CH₃). ESI-MS: *m/z* calcd (found) 919.1026 (919.1118) [M⁺ – PF₆], 624.0848 (624.0843) [M⁺ – C₆H₁₄S₂(PF₆)₂]. Elemental analysis: calcd (found) for C₃₈H₃₆F₁₂N₆O₂P₂RuS₂·H₂O; C: 42.19 (42.15), H: 3.54 (3.48), N: 7.77 (7.99). IR (cm^{−1}): 1622, 1602 (C=N), 838 (PF₆[−]), 659 (CH₂–S–CH₂), N → Ru (558).

[Ru(bpy)₂(L2)][PF₆]₂ (2). This compound was prepared following the same procedure as described above for [Ru(bpy)₂(L1)][PF₆]₂ using **L2** (75 mg, 0.20 mmol) and [Ru(bpy)₂Cl₂]·2H₂O (104 mg, 0.20 mmol). Yield: 70 mg (34%). ¹H NMR (400 MHz, CD₃CN): δ = 8.64 (dd, 2H, phen, *J*₁ = 8.5 Hz, *J*₂ = 1.2 Hz), 8.55 (dd, 4H, bpy, *J*₁ = 14.9 Hz, *J*₂ = 8.1 Hz), 8.11 (t, 2H, bpy, *J*₁ = 7.9 Hz, *J*₂ = 7.9 Hz), 8.02 (dd, 2H, bpy, *J*₁ = 7.9 Hz, *J*₂ = 7.9 Hz), 7.96 (dd, 2H, phen, *J*₁ = 5.2 Hz, *J*₂ = 1.2 Hz), 7.85 (d, 2H, bpy, *J* = 4.9 Hz), 7.55 (d, 2H, phen, *J* = 5.8 Hz), 7.47 (m, 2H, bpy), 7.26 (m, 4H, bpy), 4.44 (m, 4H, OCH₂), 2.99–2.76 (m, 8H, SCH₂); ¹³C NMR: 155.3, 152.0, 151.5, 143.8, 139.4, 137.7, 131.6, 128.4, 127.5, 127.3, 124.2 (phen/bpy); 73.4 (OCH₂), 34.2, 31.7 (SCH₂). ESI-MS: *m/z* calcd (found) 917.0870 (917.0871) [M⁺ – PF₆], 624.0848 (624.0843) [M⁺ – C₆H₁₂S₂(PF₆)₂]. Elemental analysis: calcd (found) for C₃₈H₃₄F₁₂N₆O₂P₂RuS₂·H₂O; C: 42.27 (43.13), H: 3.36 (3.78), N: 7.78 (7.55). IR (cm^{−1}): 1630, 1603 (C=N), 838 (PF₆[−]), sh (CH₂–S–CH₂), N → Ru (558).

[Ru(bpy)₂(L3)][PF₆]₂ (3). This compound was prepared following the same procedure as described above for [Ru(bpy)₂(L1)][PF₆]₂ using **L3** (90 mg, 0.21 mmol) and [Ru(bpy)₂Cl₂]·2H₂O (110 mg, 0.21 mmol). Yield: 98 mg (38%). ¹H NMR (400 MHz, CD₃CN): δ = 8.84 (m, 2H, phen), 8.54 (dd, 4H, bpy, *J*₁ = 13.3 Hz, *J*₂ = 8.1 Hz), 8.12 (dd, 2H, bpy, *J*₁ = 7.8 Hz, *J*₂ = 7.8 Hz), 8.02 (dd, 4H, bpy, *J*₁ = 9.8 Hz, *J*₂ = 4.0 Hz), 7.85 (d, 2H, phen, *J* = 5.1 Hz), 7.74 (m, 2H, bpy), 7.56 (d, 2H, phen, *J* = 5.5 Hz), 7.47 (m, 2H, bpy), 7.26 (m, 2H, bpy), 4.53 (m, 4H, OCH₂), 3.12–2.79 (m, 12H, SCH₂); ¹³C NMR: 157.0, 152.5, 151.6, 150.3, 138.1, 134.3, 132.2, 131.7, 128.1, 126.2, 124.2 (phen/bpy); 68.0 (OCH₂); 32.5, 31.7 (SCH₂). ESI-MS: *m/z* calcd (found) 977.0904 (977.0940) (M⁺ – PF₆), 624.0848 (624.0843) [M⁺ – C₈H₁₆S₃(PF₆)₂]. Elemental analysis: calcd (found) for C₄₀H₃₈F₁₂N₆O₂P₂RuS₃·H₂O; C: 42.11 (42.61), H: 3.54 (3.95), N: 7.37 (7.58). IR (cm^{−1}): 1629, 1603 (C=N), 838 (PF₆[−]), sh (CH₂–S–CH₂), N → Ru (558).

[Ru(bpy)₂(L4)][PF₆]₂ (4). This compound was prepared following the same procedure as described above for [Ru(bpy)₂(L1)][PF₆]₂ using **L4** (72 mg, 0.15 mmol) and [Ru(bpy)₂Cl₂]·2H₂O (80 mg, 0.15 mmol). Yield: 70 mg (38%). ¹H NMR (400 MHz, CD₃CN): δ = 8.91 (m, 2H, phen), 8.49 (dd, 4H, bpy, *J*₁ = 14.4 Hz, *J*₂ = 7.9 Hz), 8.12 (dd, 2H, bpy, *J*₁ = 7.8 Hz, *J*₂ = 7.8 Hz), 8.01 (m, 4H, bpy), 7.82 (m, 4H, bpy), 7.59 (m, 2H, phen), 7.53 (d, 2H, phen), 7.36 (d, 2H, bpy, *J* = 7.4 Hz), 4.51 (m, 4H, OCH₂), 3.16–2.72 (m, 16H, SCH₂); ¹³C NMR: 157.3, 151.8, 150.1, 143.3, 137.8, 134.7, 129.8, 127.5, 125.6, 125.3, 124.2 (phen/bpy); 68.9 (OCH₂), 33.4, 30.6, 30.3 (SCH₂). ESI-MS: *m/z* calcd (found) 624.0848 (624.0843) [M⁺ – C₁₀H₂₀S₄(PF₆)₂]. Elemental analysis: calcd (found) for C₄₂H₄₂F₁₂N₆O₂P₂RuS₄·H₂O; C: 42.03 (42.07), H: 3.67 (3.48), N: 7.00 (6.89). IR (cm^{−1}): 1623, 1603 (C=N), 834 (PF₆[−]), 703 (CH₂–S–CH₂), N → Ru (557).

Results and discussion

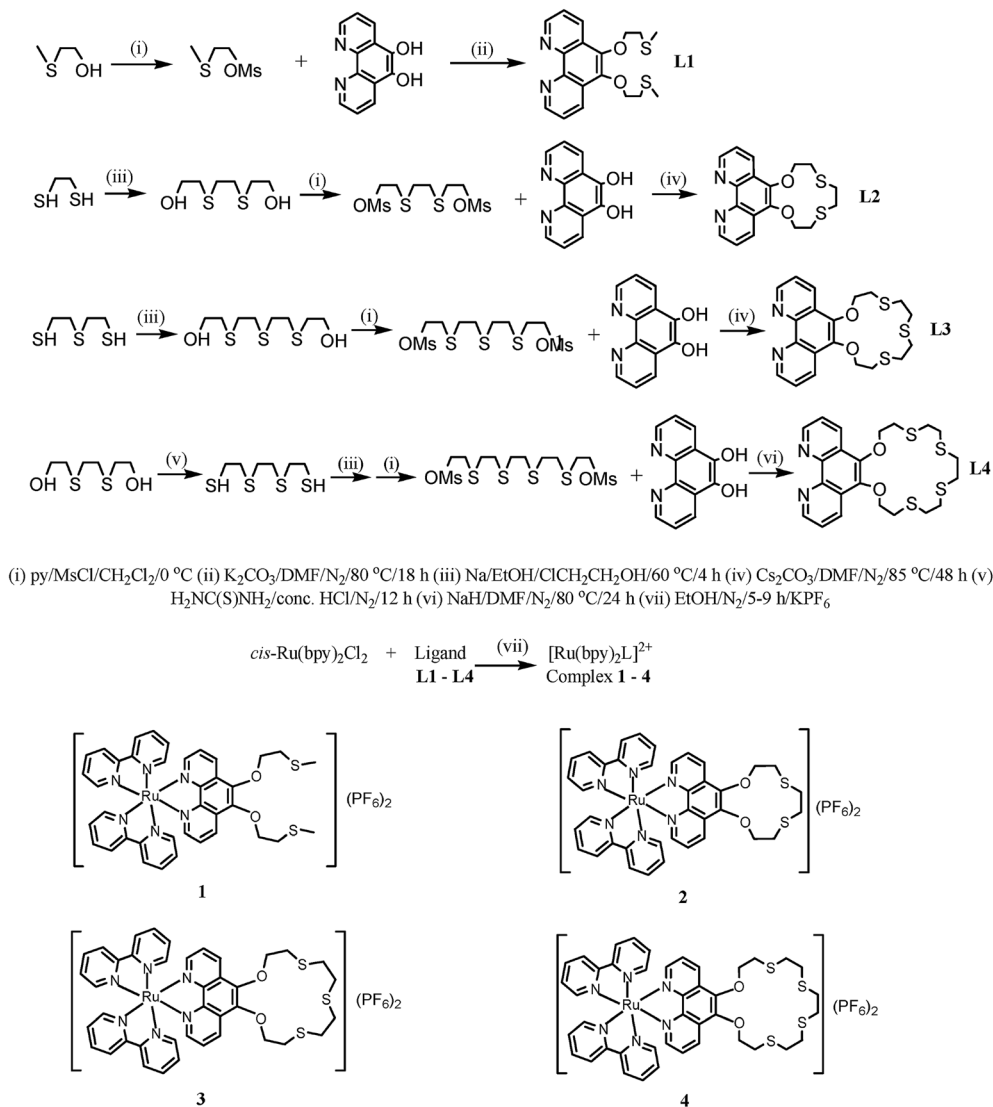
Synthesis and characterization

A new synthetic strategy for generating the oxathiacrown ether ligands is given in Scheme 1 and involved refluxing 5,6-dihydroxy-1,10-phenanthroline with the oxathia mesylate (for **L1**) or oxathia dimesylate (for **L2–L4**) in DMF under a nitrogen atmosphere. **L2** and **L3** were prepared using Schlenk line techniques. 1,10-Phenanthroline-5,6-dione¹⁸ and 5,6-dihydroxy-1,10-phenanthroline¹⁹ were prepared using established literature methods, whereas the other intermediate compounds were synthesised following modified published procedures.^{15,17} Previously, a tosylate group has been widely used as a protective group in macrocyclic synthesis and has the advantages of high stability towards harsh reaction conditions, but it leads to many undesired by-products eventually giving low yields.²⁴ Ligand **L3** was previously synthesised *via* an alternative route where 5,6-bis(2-chloroethoxy)-1,10-phenanthroline was refluxed with 2-mercaptoethyl sulphide in ethanol in the presence of NaOH, resulting in a yield of 30%.⁹ In our hands, attempts to prepare **L2** and **L3** from the reaction of 5,6-bis(2-tosylatoethoxy)-1,10-phenanthroline with the dithiols and Cs₂CO₃ under conditions of high dilution gave very low yields. A new method where the thiols are protected by the mesyl group and the corresponding dimesylates reacted with 5,6-dihydroxy-1,10-phenanthroline in DMF was therefore employed. The method involves fewer steps and gives improved yields (50–57%) of the ligands. Attempts to synthesize **L4** using Cs₂CO₃ were unsuccessful, but a yield of 43% was realised after refluxing 5,6-dihydroxy-1,10-phenanthroline and 3,6,9,12-tetrathiatetradecane-1,14-dimesylate with NaH for 24 h. Although no conditions for high dilution were used, no [2 + 2] or higher order adducts were observed in any of the reactions.

Synthesis of the ruthenium complexes **1–4** was achieved from the stoichiometric reaction of [Ru(bpy)₂Cl₂]·2H₂O with the corresponding ligand in ethanol; the complexes were precipitated with PF₆[−]. Ligand **L3** and complex **3** have been previously reported and their spectral data agree with those in the literature.⁹

The remaining ligands and complexes were characterised by ¹H NMR, ¹³C NMR and IR spectroscopy and mass spectrometry and this gave results consistent with their expected





Scheme 1 Synthesis of ligands and complexes.

formulations. In the ^1H NMR spectra of the free ligands **L1–L4**, the phen moiety exhibits its chemical shifts in the aromatic region as expected, Ar-OCH_2 protons appear in the range δ 4.60–4.38 while the SCH_2 protons of the crown ring appear in the δ 3.18–2.78 region (Fig. S1 in ESI†). In the ^1H NMR spectra of the ruthenium complexes **1–4**, the aromatic protons in the two bpy and phen rings resonate in the δ 8.93–7.26 region. Each of the bpy units however, lie in magnetically non-equivalent positions and this gives more than the four expected signals (Fig. S2 in ESI†). The aromatic proton signals of the bound ligand in the complexes however show an upfield shift by 0.10–0.63 ppm, compared to those of the corresponding free ligands. This data is in agreement with literature values of similar complexes.^{9,25} In addition, the ruthenium complexes **1–4** were characterized by elemental analysis, which indicated the presence of one molecule of water/Ru. This is in agreement with literature reports on similar complexes and was corroborated by the presence of a water peak in the ^1H NMR spectra. In all complexes, the ESI mass spectral data have a characteristic m/z

peak at 624.0843, which may be attributed to the loss of two PF_6^- anions and the thia-crown groups.

Electronic absorption and emission spectral properties

All the absorption spectra of the free ligands (**L1–L4**) in CH_2Cl_2 exhibit intense absorptions in the range ca. 230–250 nm and 270–290 nm with molar extinction coefficients in the order of 10^4 , attributable to intra-ligand, spin-allowed $n-\pi^*$ and $\pi-\pi^*$ transitions, respectively, centred on the phen unit. The corresponding complexes (**1–4**) exhibit an extra low-energy absorption band with a molar extinction coefficients in the order of 10^3 at ca. 451–457 nm. These bands which are typical of $[\text{Ru}(\text{bpy})_3]^{2+}$ moieties may be assigned to the MLCT $[\text{d}(\pi_{\text{Ru}})-\pi^*(\text{phen/bpy})]$ transitions.²⁶ A red shift of ca. $5\text{--}15\text{ cm}^{-1}$ is observed in the $\pi-\pi^*$ intra-ligand transitions in the complexes compared to the ligands. These are presumed to result from the localization of the LUMO on the phen unit whose energy is lowered upon coordinating to the metal.²⁷ No remarkable differences are observed in the absorption spectra of complexes **1–4**, showing

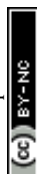


Table 1 Photophysical data, binding constant ($\log K_s$) and LOD of complexes 1–4

Complex	Absorption λ_{abs} nm ($\epsilon \times 10^4 \text{ M}^{-1} \text{ cm}^{-1}$)	Emission maxima λ_{em} (nm)	Φ_{em}^b	Lifetime τ (μs)	Metal Ion	$\log K_s$		LOD	
						UV/Vis	Emission	UV/Vis	Emission
1	243 (3.517), 288 (6.652), 456 (1.170)	611	0.012	0.139	Hg ²⁺	4.60 \pm 0.01	5.25 \pm 0.04	3.83 $\times 10^{-4}$	4.74 $\times 10^{-4}$
					Cd ²⁺	^a	5.21 \pm 0.05	^a	3.56 $\times 10^{-4}$
					Pb ²⁺	^a	^a	^a	^a
2	245 (3.428), 283 (6.322), 457 (0.943)	610	0.014	0.162	Hg ²⁺	4.72 \pm 0.01	^a	6.83 $\times 10^{-5}$	3.02 $\times 10^{-4}$
					Cd ²⁺	^a	5.38 \pm 0.01	^a	2.90 $\times 10^{-4}$
					Pb ²⁺	^a	^a	^a	^a
3	247 (3.686), 284 (6.140), 451 (1.155)	607	0.013 ^c	0.157	Hg ²⁺	^a	4.59 \pm 0.05	^a	3.79 $\times 10^{-4}$
					Cd ²⁺	^a	^a	^a	^a
					Pb ²⁺	^a	^a	^a	^a
4	244 (3.789), 287 (6.035), 453 (1.112)	608	0.011	0.133	Hg ²⁺	4.09 \pm 0.02	4.79 \pm 0.03	5.01 $\times 10^{-4}$	2.10 $\times 10^{-3}$
					Cd ²⁺	^a	4.45 \pm 0.01	^a	7.79 $\times 10^{-4}$
					Pb ²⁺	^a	^a	^a	^a

^a The spectral changes are too small for accurate determination of the binding constant. ^b The luminescence quantum yield, measured at room temperature using [Ru(bpy)₃]²⁺ as the standard. ^c A quantum yield of 0.058 in nitrogen saturated MeCN for complex 3 has been reported in literature.⁹

that electronic effects exerted by the substituents on the remote oxathiacycrown ether pendants on the phen ring are negligible. Previously, it has been shown that substituents in the 5- and/or 6-positions have negligible effects on the wavelength of absorption.^{28,29}

The luminescence spectra of the complexes were recorded in CH₃CN at room temperature with excitation at the absorption maxima (λ_{max}) of the MLCT bands. The complexes exhibit broad emission manifolds which may be assigned as ³MLCT phosphorescence, in the 607–611 nm region. These results are consistent with literature data.^{9,30} The radiative decay rate constants, k_r (where $k_r = \Phi_{\text{em}}/\tau_{\text{em}}$; Φ_{em} = quantum yield; τ_{em} = lifetime) for the ruthenium complexes fall in the 8.4–8.8 $\times 10^4 \text{ s}^{-1}$ region, typical of ³MLCT emitters whose values occur at ca. $8 \pm 4 \times 10^4 \text{ s}^{-1}$.³¹ All the complexes show similar emission properties, indicating that varying the oxathiacycrown ether cavity size does not influence their excited state energies. Luminescence quantum yields of ca. 0.012 \pm 0.002 were obtained from optically dilute samples in air-equilibrated acetonitrile, employing [Ru(bpy)₃]Cl₂ in water as the standard ($\Phi = 0.04$). These values are lower than 0.018 reported for similar complexes in air saturated acetonitrile.²¹ The complexes have lifetimes of ca. 0.13–0.16 μs . The relatively long lifetimes in solution are indicative of emissions from the lowest energy ³MLCT

excited states. These values are slightly below 0.4 μs found in similar ruthenium complexes of type [Ru(bpy)₂phen]²⁺.³² The photophysical data for the complexes are summarized in Table 1.

Electrochemical properties

Electrochemical properties of the complexes in CH₃CN solution containing 0.1 M ⁿBu₄NPF₆ as the supporting electrolyte were investigated by cyclic voltammetry. The complexes were subjected to a voltage scan from –2.2 V to 1.5 V and back at a scan rate of 100 mV s^{–1}. The data is summarized in Table 2 below while a typical cyclic voltammogram of a [Ru(bpy)₃]²⁺ derivative is shown in Fig. S3 in the ESI.†

The complexes exhibit a reversible metal-centred oxidation wave attributable to [Ru(II) \rightarrow Ru(III) + e] at 1.00–1.02 V; and the oxidation potential of complex 3 is in agreement with the literature value of 1.27 V vs. SCE⁹ [Ag/AgNO₃ (0.01 M in MeCN) vs. SCE = 0.3 V]. The peak potentials for all the complexes are however lower than the generally observed value of 1.26 V (vs. Ag/AgNO₃) for [Ru(bpy)₃]²⁺,³³ due to the presence of electron releasing thiacycrown ether substituents in the complexes. Electron-donating groups are known to facilitate the oxidation of the Ru(II) centre by pumping in electrons.³⁴ Although these are one electron transfer systems, plots of $\sqrt{(\text{scan rate})}$ vs. ΔE_p (where $\Delta E_p = E_{\text{ox}} - E_{\text{red}}$) for 1–4 show intercepts ranging between 60 and 90 mV, indicating that the oxidation process may be controlled by both diffusion and kinetic factors. A representative plot is shown in Fig. S4 in ESI.† No ligand centred oxidation potential was observed in this work, although some ruthenium polypyridyl complexes are known to display ligand oxidation around 1.24 V.²⁵

The CVs of the ruthenium complexes also show three reversible reduction peaks between –1.62 V and –2.10 V. Although reduction may involve a metal- or ligand-centred orbital depending on their relative energies, ruthenium polypyridyl complexes are known to undergo a ligand centred reduction process.²⁵ The reversible reduction waves observed in

Table 2 Electrochemical data for complexes 1–4 in acetonitrile solution^a

Complex	Oxidation: $E_{1/2}$, V (ΔE_p , mV)		Reduction: $E_{1/2}$, V (ΔE_p , mV)	
	1.02 (81)	–1.62 (67)	–1.81 (71)	–2.03 (68)
1	1.02 (81)	–1.62 (67)	–1.81 (71)	–2.03 (68)
2	1.00 (90)	–1.62 (76)	–1.81 (78)	–2.04 (73)
3	1.00 (71)	–1.64 (62)	–1.82 (64)	–2.06 (63)
4	1.00 (87)	–1.65 (84)	–1.83 (76)	–2.07 (76)

^a V vs. Ag/Ag⁺; scan rate = 100 mV s^{–1}, $\Delta E_p = |E_{\text{pa}} - E_{\text{pc}}|$ while $E_{1/2} = (E_{\text{pa}} + E_{\text{pc}})/2$.



this study may thus be attributed to the addition of electrons into the π^* -orbitals of the ligand. It is noteworthy that the reduction processes of heteroleptic ruthenium polypyridyl complexes may be explained by a 'localization model' where each reduction step is attributed to one or several finite ligands.³³ The reduction peaks observed at -1.63 to -1.65 V and -1.82 to -1.84 V may thus point to the sequential one-electron reduction of the bpy ligands, $[\text{bpy} \rightarrow \text{bpy}^-]$, consistent with literature^{9,35} while the third reduction peak at -2.05 to -2.10 V may be associated with the phen unit, as confirmed by Lazarides and co-workers.³⁶ As the macrocyclic cavity increases from **L2**–**L4**, an anodic shift of 10–30 mV is observed in the ligand reduction potentials and the ease of reduction follows the **L2** > **L3** > **L4** order. The substituents directly attached to phen pump electrons into the π^* orbital of bpy/phen moieties and hence make reduction process harder. The shifts are however too small to affect the $d\pi$ – π^* separation which has a direct correlation with $E_{\text{ox}} - E_{\text{red}}$. Generally, substituents in the 5- and/or 6-position of the 1,10-phenanthroline have a lesser influence and hence a lower energy gap than when they occupy a position in the N-containing rings.²⁸

Sensitivity and selectivity studies

The sensitivity and selectivity of the oxathia crown ether ruthenium complexes for Hg^{2+} , Cd^{2+} and Pb^{2+} ions were investigated by titrating the complexes **1**–**4** with the metal ions (0–10 equiv.) and monitoring the electronic absorption, luminescence and electrochemical changes.

Electronic absorption titrations

The complexes **1**–**4** were titrated with 0–10 equiv. of Hg^{2+} , Cd^{2+} and Pb^{2+} ions in acetonitrile at room temperature and their spectra recorded. On adding Hg^{2+} ions to **1**, **2** and **4**, perturbed absorption spectra are observed with the peak at ca. 457 nm diminishing as a new peak forms at ca. 427 nm. The perturbation points to the formation of 1-Hg^{2+} , 2-Hg^{2+} and 4-Hg^{2+} complexes in the ground state. The binding of the Hg^{2+} by the receptor leads to a reduction of the electron-donating ability of the oxathia crown ether conjugated to the phen unit, resulting in a 30 nm blue shift of the absorbance and hence a high selectivity for Hg^{2+} . Three clear isosbestic points are observed at 442, 380 and 323 nm (Fig. 1).

These isosbestic points indicate the presence of two absorbing species (the free and the bound host complex) at equilibrium in solution. The absorption spectrum of complex **3**, on the other hand, is unperturbed by the presence of Hg^{2+} ions. This is in agreement with the literature⁹ and may point to a different binding mode in the macrocyclic cavity. The interaction of Hg^{2+} with the complexes is also clearly observable by the naked eye as a colour change from red-orange to yellow as shown in Fig. 2.

Titration of **1**–**4** with Cd^{2+} and Pb^{2+} ions display insignificant spectral changes, hence absorbance changes can be used to selectively identify Hg^{2+} over the other ions since it is the only metal ion that changes the absorption spectra.

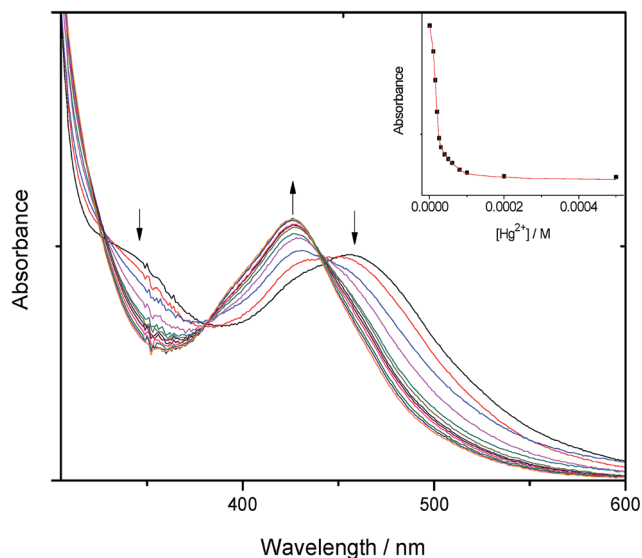


Fig. 1 Absorption titration spectra of **2** (5×10^{-5} M) with added Hg^{2+} (0 – 2×10^{-4} M) in CH_3CN at room temperature. Inset: a plot of absorbance vs. $[\text{Hg}^{2+}]$ at 500 nm. $R^2 = 0.995$.

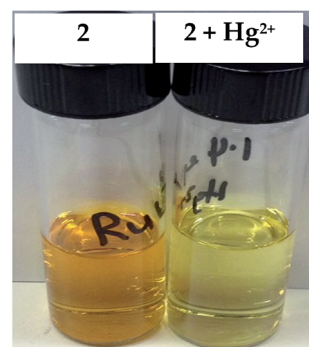


Fig. 2 Color change showing the interaction between complex **2** and Hg^{2+} ions.

Emission titrations

The emission responses of the complexes **1**–**4** upon addition of Hg^{2+} , Cd^{2+} and Pb^{2+} ions were investigated in acetonitrile solution at room temperature. Addition of Hg^{2+} to complexes **1** and **4** result in a 10–26% peak enhancement. The strong interaction between the metal ion and the thiacycrown ether moiety makes the latter a poor electron donor to quench the emissive $^3\text{MLCT}$ state, thus resulting in enhancement of the emission intensity.¹⁵ The peak enhancement continues until the right stoichiometric amounts of the metal ions and the complexes have reacted together. Although **2** shows a general peak enhancement, the luminescence spectra display some irregular behaviour. Upon adding Hg^{2+} (initially upto 0.5 equiv.), a peak enhancement (18%) is observed at 610 nm, followed by a gradually decreasing red shifted emission maximum at 615 nm (Fig. S5 in the ESI†). Similar unusual observations have been made with some crown moieties.²²

The interaction of Hg^{2+} with **3** displays a 25% quenching of the ruthenium peak at 1 : 1 stoichiometric addition. Although



a 40% quenching of the same complex with Hg^{2+} has been previously reported in literature,⁹ its quenching mechanism was never investigated. A Stern–Volmer plot of I_0/I vs. $[\text{Hg}^{2+}]$ (where I_0 = initial emission intensity of the ruthenium complex without Hg^{2+} , I = emission intensity at a given $[\text{Hg}^{2+}]$) gives a downward curvature concave towards the x-axis. This negative deviation from linearity represents a quenching that is not purely collisional. Although negative deviation may be attributed to ground state complex formation, this is unlikely in the 3- Hg^{2+} interaction since the absorbance plot is unperturbed. It is however reasonable to assume that Hg^{2+} reacts with a photo-activated 3 complex to form a new activated species which emits light of energy distribution for both the radiative and non-radiative pathways, different from that emitted by the original 3. Another possible explanation for the negative shift is the fact that binding of Hg^{2+} to 3 may effect conformational changes on the chromo-ionophore, thus giving rise to a weakly emissive excited state. Similar observations have been noted in other chromo-ionophores.⁶ Although the fluorescence spectra should in principle be shifted in the same direction as those of the absorption spectra,³⁷ this is not observed when Hg^{2+} interacts with complexes 1–4. While the absorption spectra of 1, 2 and 4 are blue shifted by ca. 30 nm, the corresponding luminescence spectra including that of 3 are red shifted by ca. 5 nm. The anomaly may be caused by changes in the charge–dipole interaction of Hg^{2+} and the positively charged ruthenium(II) centre in the excited state which results in a decrease in the emission energy.

On titrating 1–4 with Cd^{2+} , peak enhancement of 30, 54 and 15% are observed with 1, 2 and 4 respectively while 3 trails at 7%. The highest peak enhancement of 54% with 2 is indicative of the optimal chromo-ionophoric cavity size for the Cd^{2+} ions. Cd^{2+} has borderline hard and soft acid properties and hence it binds well within the oxathia crown ether moiety. Although 4, has a bigger macrocyclic cavity compared to 3, its peak enhancement is higher probably due to the fact that it can accommodate two Cd^{2+} ions (the binding isotherm is 1 : 2) as opposed to 3 whose binding isotherm is 1 : 1. Sequential addition of Pb^{2+} ions to 1–4 generally leads to an insignificant peak enhancement of 6 to 8%, with a saturation threshold at 8 equiv. Hence, using luminescence, 3 is selective towards Hg^{2+} while 2 is selective towards Cd^{2+} . None of the complexes appears to be selective towards Pb^{2+} ions.

Electrochemical titrations

The electrochemical response of the oxidation potential of Ru(II) in the presence of Hg^{2+} , Cd^{2+} and Pb^{2+} was investigated by means of cyclic voltammetry (CV) and differential pulse voltammetry (DPV). Upon sequential addition of Hg^{2+} ions to complex 3, an anodic shift of the ruthenium(II) oxidation peak potential by 20 mV and an 11% decrease in peak current were observed. This anodic shift may be attributed to the electron-withdrawing effect of the positively charged metal-complexed thia-crown ether moiety which causes the ruthenium to oxidize at a more positive potential. Anodic shifts have been reported in ruthenium polypyridyl complexes attached to

calixarenes when they bind Na^+ , Hg^{2+} and Pb^{2+} ions.¹⁵ The rest of the complexes (1, 2 and 4 with Hg^{2+} and 1–4 with Cd^{2+} and Pb^{2+}) don't display any significant shifts in the oxidation peak potential of the ruthenium(II) centre using neither CV nor DPV. This may indicate a weak or non-existing effective electrochemical communication between the ruthenium(II) centre and the metal-bound thia-crown ether moiety, as far as electrochemistry is concerned.³⁸

Binding constant

The binding constants ($\log K_s$) shown in Table 1 were determined from the changes recorded in the luminescence or absorbance titrations at appropriate wavelengths where the variations are as large as possible. From luminescence spectral data, the binding constant was obtained following literature method²² in accordance with eqn (1):

$$\frac{I_0 - I}{I - I_\infty} = \left\{ \frac{[M]}{K_{\text{diss}}} \right\}^n \quad (1)$$

where I_0 and I represent the initial emission intensity of the host complex in the absence of the metal ions and at a metal ion concentration $[M]$ respectively. I_∞ is the emission intensity at maximum concentration of metal ion when no further change in emission intensity takes place. A double logarithmic plot of $\log[(I_0 - I)/(I - I_\infty)]$ vs. $\log[M]$ is a straight line whose slope gives the value of n , which represents the number of guest ions bound to the host complex, whereas the value of $\log[M]$ at $\log[(I_0 - I)/(I - I_\infty)] = 0$ (i.e. y-intercept) gives the value of $\log K_{\text{diss}}$ whose reciprocal is the binding constant (K_s). Binding constants were also obtained from absorbance spectral data by modifying eqn (1) above into eqn (2).

$$\frac{A_0 - A}{A - A_\infty} = \left\{ \frac{[M]}{K_{\text{diss}}} \right\}^n \quad (2)$$

where A_0 and A are the absorbance of the complex at a selected wavelength in the absence and presence of the guest metal ion respectively. A_∞ is the limiting value of the absorbance in the presence of excess metal ion. A representative plot is shown in Fig. S6 in ESI.†

Using luminescence, 2 shows a relatively high binding constant with Cd^{2+} due to its optimal cavity size for the cation while 4 shows a lower binding constant. This may be attributed to the binding stoichiometry of 1 : 1 in 2: Cd^{2+} which results in a stronger binding compared to a 1 : 2 binding model in 4: Cd^{2+} . The binding constant in 2: Cd^{2+} also appears higher than 1: Cd^{2+} due to macrocyclic effect which enhances the stability of the complex formed. Using absorbance, the spectral changes were too small for accurate determination of $\log K_s$. The binding constants for 1: Hg^{2+} and 4: Hg^{2+} determined from the luminescence spectral data are slightly higher than those determined from UV-Vis data, but there may be some underestimation of the errors. Overall it seems that luminescence measurements are more sensitive in the determination of the binding constants of the metal ions in the thiacycrown ethers. $\log K_s$ obtained from 3: Hg^{2+} is comparable with the literature value.⁹ It was not possible to calculate the binding constant in



2:Hg^{2+} using luminescence due to the irregular behaviour of the spectra. The binding constants of **1–4** with Pb^{2+} were not determined because the spectral changes are too small for accurate determination of the K_s values.

Limit of detection

The limit of detection was calculated using the standard deviation method³⁸ expressed in eqn (3):

$$\text{LOD} = \frac{3.3 \times \text{standard deviation of the regression line of conc. vs. } A \text{ or } I}{\text{Slope}} \quad (3)$$

From the calculations, complex **2** shows the lowest detection limit of 68 ppm towards Hg^{2+} using absorbance. While the rest of the complexes [**1**, **3** and **4**] detect Hg^{2+} or Cd^{2+} at higher concentrations *ca.* 0.2–0.8 millimolar using luminescence (*cf.* Table 1).

Interference studies

The responses of the complexes **1–4** towards various mono- and divalent cations (Li^+ , Na^+ , K^+ , Ag^+ , Ca^{2+} , Mg^{2+} , Cu^{2+} and Zn^{2+}) and anions (Cl^- , Br^- , I^- , NO_3^- , OAc^- , ClO_4^- , HSO_4^- and HPO_4^-) were investigated by adding 10 equivalent of each ion and noting the spectral changes. The absorbance of the ruthenium peak displays negligible changes upon adding 10 equiv. of the various guest metal ions under investigation. Electronic absorption responses of complex **2** to the addition of 10 equiv. of various metal ions is shown in Fig. 3.

Generating a ratiometric signal by calibrating absorption bands at 457 nm and 427 nm for **1**, **2** and **4** help eliminate most ambiguous responses to the presence of Hg^{2+} ions. A typical graphical representation of the ratiometric signals of absorbance at 427 nm/457 nm is shown in Fig. S7 (ESI[†]). On adding 10 equiv.

of various anions to all the complexes **1–4**, the ruthenium peak appears unperturbed (Fig. S8 in ESI[†]).

Using luminescence, ruthenium peak enhancements (0 ≤ 10%) are noted on adding 10 equiv. of various guest cations with no particular trend observed with **1** and small effects with **2**. Complexes **3** and **4** exhibit an interesting behaviour with the monovalent cations displaying no effect and the divalent cations showing a peak enhancement of 8 to 10%. This enhancement may be attributed to the strong interaction between divalent cations and the lone pair of electrons on the oxygen atom attached to the phen unit, making it a poor donor to quench the emissive triplet $^3\text{MLCT}$ state. The small effect on the ruthenium peak by the monovalent cations may be due to weak interactions between the +1 charge and lone pair of electrons on oxygen. Cu^{2+} generally shows a quenching of *ca.* 8% with all the ruthenium complexes. Representative spectra showing the effect of various guest cations on **3** is displayed in Fig. S9 (ESI[†]) while a graphical representation of the responses of complexes **1–4** to the addition of all the metal ions under investigation is shown in Fig. S10 (ESI[†]). On adding 10 equiv. of each of the guest anions under investigation to the complexes, the NO_3^- anion shows a peak enhancement of 6 to 12% while the other anions have no effect.

Conclusion

A series of ruthenium(II) complexes attached to oxathia-crown ether pendants have been synthesized and characterized. Their recognition properties towards Hg^{2+} , Cd^{2+} and Pb^{2+} have been investigated by spectroscopic and electrochemical means. The ruthenium complexes **1**, **2** and **4** display selectivity towards Hg^{2+} using electronic absorption spectra. By calibrating their two absorption bands at 457 nm and 427 nm, a ratiometric signal may be generated, and this can eliminate most ambiguities from interfering ions. However, **2** would be a more suitable excellent probe for Hg^{2+} detection than **1** and **4** using absorbance detection due to its low detection limit and colorimetric changes that can be observed by the naked eye. Using luminescence, complex **2** is selective towards Cd^{2+} with a binding constant of $\log 5.38$ and LOD of 2.9×10^{-4} . Complex **3** is selective towards Hg^{2+} even though it has a relatively lower binding constant and higher LOD. None of the ruthenium complexes is selective towards Pb^{2+} ions. Although the thia-crown has a high affinity for the softer Hg^{2+} ions, the spectral changes and hence the binding constants obtained are lower than expected. This is due to their remoteness from the phen unit and hence little influence on the π^* energy orbital of the phen ligand. Electrochemically, none of the complexes is able to recognize the presence of the guest metal ions due to lack of effective electronic communication between the ruthenium metal centre and the phen-ligand. As the macrocyclic cavity increases from complex **2–4**, no obvious trend is observed in the spectroscopic and electrochemical responses to the presence of Hg^{2+} ions. However in the ligands, an anodic shift of 10–30 mV is observed in the ligand reduction potentials from **L2–L4** and the ease of reduction follows the **L2** > **L3** > **L4** order. The substituents directly attached to phen pump electrons into the π^* orbital of bpy/phen moieties and hence make reduction process harder.

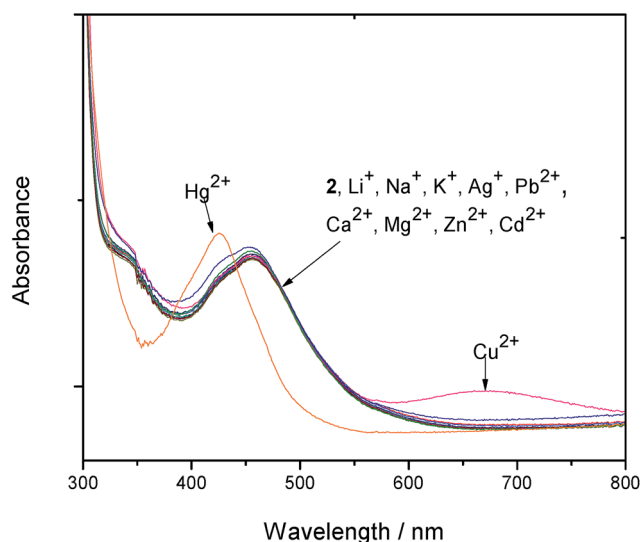


Fig. 3 UV-Vis responses of complex **2** towards the addition of 10 equiv. of various metal ions.



Conflicts of interest

There are no conflicts to declare.

Acknowledgements

We gratefully acknowledge the financial support from ISP, IFS, L'Oreal-UNESCO and NACOSTI. We also thank Lund University and the Swedish Research Council for financial support.

References

- 1 P. A. Lieberzeit and F. L. Dickert, *Anal. Bioanal. Chem.*, 2007, **387**, 237–247.
- 2 M. R. Knecht and M. Sethi, *Anal. Bioanal. Chem.*, 2009, **394**, 33–46.
- 3 C. Lodeiro and F. Pina, *Coord. Chem. Rev.*, 2009, **253**, 1353–1383.
- 4 J. Wu, W. Liu, J. Ge, H. Zhang and P. Wang, *Chem. Soc. Rev.*, 2011, 3483–3495.
- 5 V. I. Minkin, A. D. Dubonosov, V. A. Bren and V. A. Tsukanov, *ARKIVOC*, 2008, (iv), 90–102.
- 6 E. N. Ushakov, M. V. Alfimov and S. P. Gromov, *Macrocyclics*, 2010, **3**, 189–200.
- 7 V. Lippolis and M. Shamsipur, *J. Iran. Chem. Soc.*, 2006, **3**, 105–127.
- 8 H. J. Hartigan, G. Seeber, A. R. Mount, L. J. Yellowlees and N. Robertson, *New J. Chem.*, 2004, **28**, 98–103.
- 9 M.-J. Li, B. W.-K. Chu, N. Zhu and V. W.-W. Yam, *Inorg. Chem.*, 2007, **46**, 720–733.
- 10 D. J. Stewart, P. E. Fanwick and D. R. McMillin, *Inorg. Chem.*, 2010, **49**, 6814–6816.
- 11 S.-H. Fan, A.-G. Zhang, C.-C. Ju, L.-H. Gao and K.-Z. Wang, *Inorg. Chem.*, 2010, **49**, 3752–3763.
- 12 A. A. Marti, C. A. Puckett, J. Dyer, N. Stevens, S. Jockusch, J. Ju, J. K. Barton and N. J. Turro, *J. Am. Chem. Soc.*, 2007, **129**, 8680–8681.
- 13 F. Gao, X. Chen, F. Zhou, L. P. Weng, L. T. Guo, M. Chen, H. Chao and L. N. Ji, *Inorg. Chim. Acta*, 2011, **370**, 132–140.
- 14 J. Buter and R. M. Kellogg, *Org. Synth.*, 1987, **1993**(8), 592.
- 15 R. E. Wolf, J. R. Hartman, J. M. E. Storey, B. M. Foxman and S. R. Cooper, *J. Am. Chem. Soc.*, 1987, **109**, 4328–4335.
- 16 T. F. Baumann, J. G. Reynolds and G. A. Fox, *J. Chem. Soc., Chem. Commun.*, 1998, 1637.
- 17 M. Tanaka, M. Nakamura, T. Ikeda, K. Ikeda, H. Ando, Y. Shibutani, S. Yajima and K. Kimura, *J. Org. Chem.*, 2001, **66**, 7008–7012.
- 18 M. Yamada, Y. Tanaka, Y. Yoshimoto, S. Kuroda and I. Shima, *Bull. Chem. Soc. Jpn.*, 1992, **65**, 1006–1011.
- 19 W. Paw and R. Eisenberg, *Inorg. Chem.*, 1997, **36**, 2287–2293.
- 20 P. A. Lay, A. M. Sargeson, H. Taube, M. H. Chou and C. Creutz, *Inorg. Synth.*, 1986, **24**, 291–299.
- 21 K. Suzuki, A. Kobayashi, S. Kaneko, K. Takehira, T. Yoshihara, H. Ishida, Y. Shiina, S. Oishi and S. Tobita, *Phys. Chem. Chem. Phys.*, 2009, **11**, 9850–9860.
- 22 S. Patra and P. Paul, *Dalton Trans.*, 2009, 8683–8695.
- 23 S. Saravanan, T. Sudha and B. Surendra, *Drug Dev. Ther.*, 2014, **5**, 109–114.
- 24 M. W. Glenny, M. Lacombe, J. B. Love, A. J. Blake, L. F. Lindoy, R. C. Luckay, K. Gloe, B. Antonioli, C. Wilson and M. Schroder, *New J. Chem.*, 2006, **30**, 1755–1767.
- 25 X.-J. Yang, C. Janiak, J. Heinze, F. Drepper, P. Mayer, H. Piotrowski and P. Klufers, *Inorg. Chim. Acta*, 2001, **318**, 103–116.
- 26 F. Cheng, N. Tang, P. Liu, N. Hou and G. Chen, *Transition Met. Chem.*, 2012, **37**, 249–255.
- 27 C. Goze, N. Dupont, E. Beitler, C. Leiggenger, H. Jia, P. Monbaron, S.-X. Liu, A. Neels, A. Hauser and S. Decurtins, *Inorg. Chem.*, 2008, **47**, 11010–11017.
- 28 L. Wallace and D. P. Rillema, *Inorg. Chem.*, 1993, **32**, 3836–3843.
- 29 D. Schallenberg, A. Neubauer, E. Erdmann, M. Tanzler, A. Villinger, S. Lochbrunner and W. Seidel, *Inorg. Chem.*, 2014, **53**, 8859–8873.
- 30 Y. Chen, X. Zhou, X.-H. Wei, B.-L. Yu, H. Chao and L.-N. Ji, *Inorg. Chem. Commun.*, 2010, **13**, 1018–1020.
- 31 K. K.-W. Lo, M.-W. Louie and K. Y. Zhang, *Coord. Chem. Rev.*, 2010, **254**, 2603–2622.
- 32 S. Ji, W. Wu, P. Song, K. Han, Z. Wang, S. Liu, H. Guo and J. Zhao, *J. Mater. Chem.*, 2010, **20**, 1953–1963.
- 33 A. Juris and V. Balzani, *Coord. Chem. Rev.*, 1998, **84**, 85–277.
- 34 C. M. Elliott and E. J. Hershenhart, *J. Am. Chem. Soc.*, 1982, **104**, 7519–7526.
- 35 V. P. Boricha, S. Patra, Y. S. Chouhan, P. Sanavada, E. Suresh and P. Paul, *Eur. J. Inorg. Chem.*, 2009, 1256–1267.
- 36 T. Lazarides, T. A. Miller, J. C. Jeffrey, T. K. Ronson, H. Adams and M. D. Ward, *Dalton Trans.*, 2005, 528–536.
- 37 Z. Xu, Y. Xiao, X. Qian, J. Cui and D. Cui, *Org. Lett.*, 2005, **7**, 889–892.
- 38 A. K. Bilakhiya, B. Tyagi and P. Paul, *Polyhedron*, 2000, 1233–1243.

